Biosensing and Study of Biological Cells using Hyperpolarized 129 Xe

Patrick Berthault, Céline Boutin

▶ **To cite this version:**

Patrick Berthault, Céline Boutin. Biosensing and Study of Biological Cells using Hyperpolarized 129 Xe. Meersmann, T. Brunner, E. New Developments in NMR, 14, RCS, 2015, Hyperpolarized Xenon-129 Magnetic Resonance: Concepts, Production, Techniques and Applications, 978-1-84973-889-7. 10.1039/9781782628378-00261 . cea-01257658

HAL Id: cea-01257658

https://hal-cea.archives-ouvertes.fr/cea-01257658

Submitted on 18 Jan 2016

HAL is a multi-disciplinary open access archive for the deposit and dissemination of scientific research documents, whether they are published or not. The documents may come from teaching and research institutions in France or abroad, or from public or private research centers.

L'archive ouverte pluridisciplinaire **HAL**, est destinée au dépôt et à la diffusion de documents scientifiques de niveau recherche, publiés ou non, émanant des établissements d'enseignement et de recherche français ou étrangers, des laboratoires publics ou privés.

CHAPTER 14

Biosensing and Study of Biological Cells using Hyperpolarized ^{129}Xe

PATRICK BERTHAULT* AND CÉLINE BOUTIN

CEA Saclay, IRAMIS, NIMBE, UMR CEA/CNRS 3685, Laboratoire Structure et Dynamique par Résonance Magnétique, 91191 Gif sur Yvette, France
*Email: patrick.berthault@cea.fr

14.1 Introduction

Among the species in which nuclear spin can be transiently polarized, xenon has a special place for the study of biological processes due to its physical properties. It has no toxicity, it can be easily handled due to a freezing point at 162 K. Importantly, its large electron cloud gives this atom specific chemical affinities, and a large variability of its NMR parameters: the chemical shift of the monoatomic species has been shown to span a range from 0 ppm (gas phase) to 300 ppm (solid phase[1]), longitudinal relaxation time values range from *ca.* 5 seconds (xenon in blood[2]) to several hours. Its solubility in many biological fluids (a few mM per atm in water at room temperature, hundreds of mM in lipids) makes it a powerful spy of biological events.

In the aim of characterizing biological environments and events, xenon can be used alone, or functionalized by dedicated molecular systems for which it has a high affinity. These systems bear ligands that enable active targeting of biological receptors. This chapter aims at summarizing some of

New Developments in NMR No. 4
Hyperpolarized Xenon-129 Magnetic Resonance: Concepts, Production, Techniques and Applications
Edited by Thomas Meersmann and Eike Brunner
© The Royal Society of Chemistry 2015
Published by the Royal Society of Chemistry, www.rsc.org

the recent research and development we have developed using free hyperpolarized xenon and xenon in molecular hosts to image or characterize biological cell receptors.

14.2 Hyperpolarized Xenon and Biological Cells

The first experiments dealing with hyperpolarized xenon and biological cells were performed in 1995 by Albert *et al.*[2] They showed that xenon in the presence of red blood cells (RBC) gave rise to two signals on the NMR spectrum (one assigned to xenon in the plasma and the other one to xenon in RBC) exhibiting different longitudinal relaxation times. Bifone *et al.*[3] attributed the 20–24 ppm chemical shift difference between the two signals to the interaction between xenon and hemoglobin present in the intracellular compartment of RBC, the paramagnetism of this protein being in large part responsible for the chemical shift variation. The variation of the chemical shift difference and relaxation time was later correlated to the oxygenation level of hemoglobin.[4]

Recently, prokaryotic, eukaryotic cells, mammalian, vegetal, and yeast cells were studied in the presence of hyperpolarized xenon (Figure 14.1), and the presence of two signals on the ^{129}Xe NMR spectrum could be systematically observed, even in the absence of a known paramagnetic system: one signal at lower magnetic field corresponding to xenon in the intracellular compartment and the second one to xenon in the bulk.[5] This means that xenon crosses the plasma membrane while keeping its polarization and that the exchange rate between both compartments is lower than the frequency difference between both environments. Recently it has thus been pointed out that each cell type has its own signature on the ^{129}Xe NMR spectrum. As expected, the area of the signal of xenon in the inner compartment is directly proportional to the number of cells, and the presence of a mixture of cells can straightforwardly be detected, as well as the cell uptake of toxics.

But undoubtedly the most important point is that the presence of distinct signals for the inner compartment and the bulk enables measurement of the xenon in–out exchange rate with simple ^{129}Xe NMR experiments. This gives direct access to parameters usually difficult to obtain: the fluidity and permeability of the cell membrane.

We used this property for different applications, among which the most striking was the recognition of cells resistant to chemotherapy.[6]

Most of the chemotherapeutic agents are small hydrophobic molecules that cross the cell membrane in a passive (energy-free) way based on a concentration gradient. But some cells, have developed a membrane transporter system, notably *via* p-glycoprotein (Pgp),[7] in order to favor expelling of the cytotoxic drugs to the external medium. Whereas cell permeability to water is now well measured and understood, few methods are proposed to evaluate cell permeability to hydrophobic drugs.[8] The *in vitro* techniques used so far are, for example, based on the detection of the internalization of small hydrophobic fluorophores such as rhodamine 123,[9] and PCR

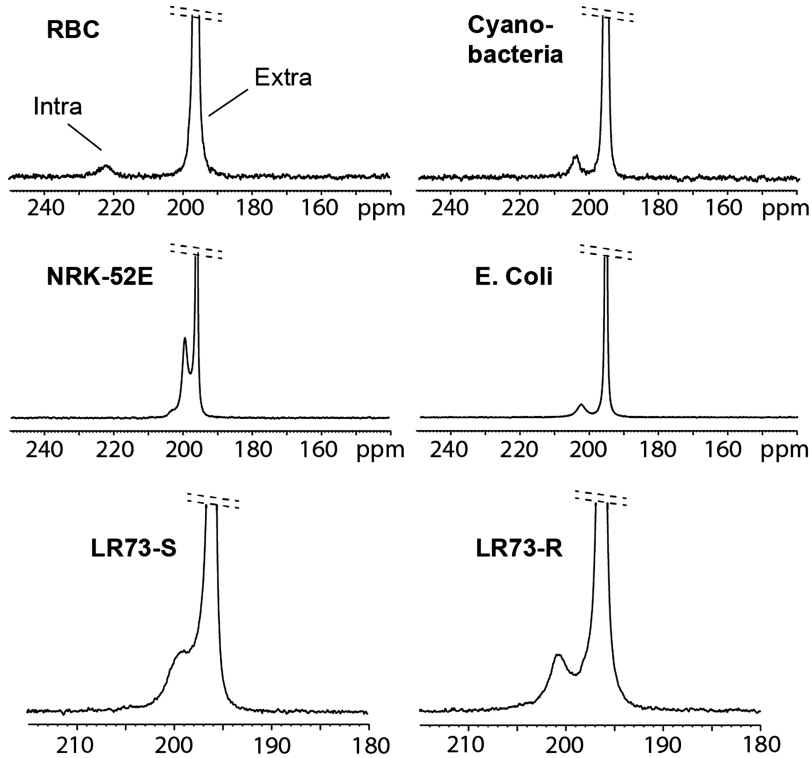

Figure 14.1 ^{129}Xe NMR spectra obtained for suspensions of different living cell types. The samples contained red blood cells, *Synechocystis* cyanobacteria, NRK-52E renal proximal cells, *Escherichia coli* TOP10 bacteria and Chinese Hamster Ovary LR73 cell lines (left: sensitive to chemotherapy; right: resistant to chemotherapy. See text).

methods[10] which witness the presence and activity of p-glycoprotein. These techniques are slow as they require an incubation delay. There is thus a real need for fast evaluation of cell permeability.

In our proof-of-concept, two Chinese Hamster Ovary cell lines were used: the wild type (LR73-S) sensitive to chemotherapeutic drugs, and the multidrug resistant type derived from it (LR73-R). This system had already been used several times as a model for studying cell drug resistance *via* Fourier transform infrared spectroscopy[11] and fluorescence correlation spectroscopy.[12] While after trypsination, classical optical microscopy did not allow us to discriminate LR73-S and LR73-R cells from their size or aspect, their one-scan ^{129}Xe NMR spectra recorded in the same conditions (same temperature, same amount of xenon and number of cells) revealed two immediate differences (Figure 14.1): (i) for the same number of cells, the ratios R between the signal areas of the inner and outer compartments differed by a factor 3.3 (see Table 14.1): the number of xenon atoms internalized per cell was in our experimental conditions more than three times

Table 14.1 Results of the ^{129}Xe NMR experiments in terms of chemical shift difference, integral ratio (cell/bulk) R and xenon in- and out-exchange rates for four different cell samples.

Sample[a]	δ splitting[b] (ppm)	Integral ratio R (cell/bulk)[b]	k_{out}/s^{-1}	k_{in}/s^{-1}
LR73-S	3.00 ± 0.21	0.561 ± 0.022	29.4 ± 5.7	16.5 ± 3.8
LR73-R	4.46 ± 0.05	0.167 ± 0.066	86.5 ± 16.7	14.4 ± 6.3
LR73-S + CsA[c]	3.00 ± 0.10	0.168 ± 0.024	32.2 ± 27.6	5.4 ± 2.3
LR73-R + CsA[c]	2.70 ± 0.04	0.113 ± 0.038	28.9 ± 7.8	3.2 ± 2.8

[a]The data of the first two rows were obtained with 10^8 cells, those of rows 3 and 4 with 4×10^7 cells (explaining the differences in R value).
[b]The measures were performed on 5 different replicate samples. The error corresponds to standard deviation. The signals in the high field regions of the ^{129}Xe spectra were fitted by Lorenzians. After all these experiments, it was checked by colorimetric trypan blue exclusion test that the cells were still alive.
[c]CsA: cyclosporin-A.

more elevated in the sensitive cell line than in the resistant cell line; (ii) the chemical shift difference significantly varied between the two cell lines: the inner xenon signal for the resistant cell line was low-field shifted by about 1.5 ppm with respect to the signal from sensitive cells. The observed chemical shift variation can be explained by the difference of plasma membrane structure, due to the over-expression of p-glycoprotein, which organizes its own micro-environment.[13]

However as variation of the xenon chemical shift could also be due to the presence of toxics or of other paramagnetic proteins, we undertook the measurement of a third parameter: the xenon exchange rate across the cell membrane. This was performed *via* a simple 1D NMR experiment consisting of selective inversion of the xenon signal in the cell and acquisition after a variable delay (Figure 14.2).

The last two columns of Table 14.1 give the exchange rates of xenon in and out of the cells. The xenon *out* rate was three times more elevated for the resistant cell line than for the sensitive cell line, whereas the *in* rates were similar. It is worth mentioning that in principle there is no direct correlation between xenon *out* rate and drug resistance, as the noble gas has no role in the cell metabolism. But xenon seems to be assimilated to a small hydrophobic molecule, recognized as such by the cells and thus behaves similarly as some anticancer drugs or antibiotics with respect to trans-membrane exchange mechanisms. An elevated xenon efflux rate thus seems to be the signature of the mechanism of active elimination of cytotoxic molecules at the origin of resistance to drugs. Such a marked difference in xenon-*out* rate could be explained by a pronounced action of p-glycoprotein, and anyway represents a very efficient way to discriminate resistant and sensitive cell lines.

In order to assess the validity of our interpretation, the effect of cyclosporine-A (CsA), a revertant agent was tested. CsA is known to interact with p-glycoprotein and to block its action. The same ^{129}Xe NMR experiments were performed in two other cell samples of LR73-S and LR73-R

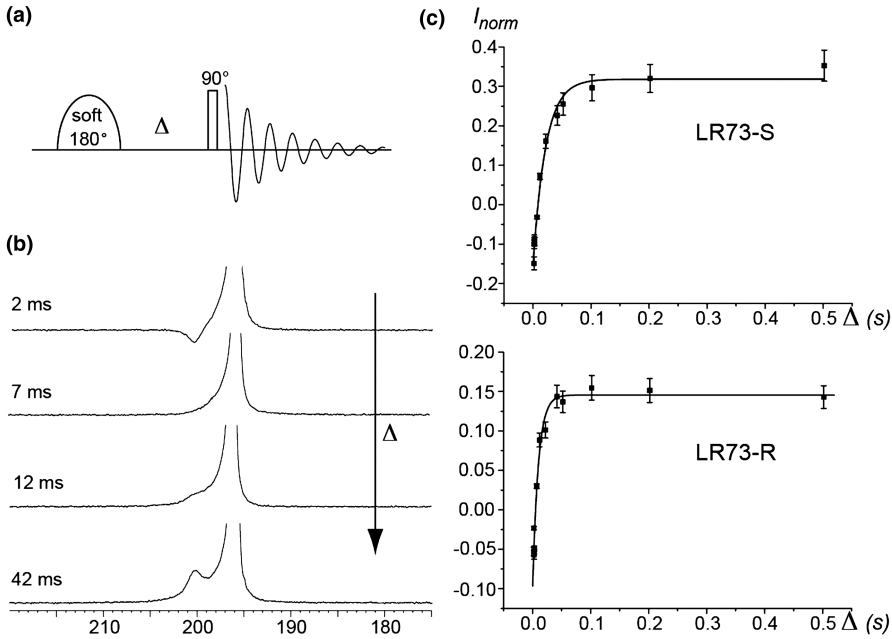

Figure 14.2 Measurement of the xenon in–out exchange rates. (a) NMR sequence. (b) Hyperpolarized ^{129}Xe NMR spectra obtained for various delays Δ on a sample of LR73-R cells. (c) Result of the exchange experiment: normalized area of the intra-cell signal as a function of Δ for LR73-S and LR73-R cell lines. The curves represent the best fit to the theoretical equation $A - B\ \exp(-k\Delta)$, where $k = k_{in} + k_{out}$. For extracting k_{in} and k_{out}, we used $R = k_{in}/k_{out}$.

cell lines incubated with cyclosporine-A. The ^{129}Xe NMR parameters for the LR73-S cells were not significantly affected by the incubation. But remarkably the characteristics of the spectrum of the LR73-R sample were now close to these of the sensitive cell sample: smaller chemical shift difference, higher number of internalized xenon atoms per cell and xenon out rate lower than without cyclosporine-A (compare lines 2 and 4 of Table 14.1). This experiment was repeated several times with different cell concentrations (from 10 to 150 million in 530 μL solution), and gave similar results. Obviously the higher xenon *out* rate for cells resistant to chemotherapy combined with a constant – but cell concentration dependent for a given quantity of noble gas – xenon *in* rate led to a lower ratio R between the signal areas of the inner and outer compartments.

As far as we know, no other NMR method exists for the determination of the permeability of the cell membrane to hydrophobic molecules. The proposed method is quick and straightforward, and does not require the use of a model. It only needs a high field NMR spectrometer or imager equipped with a standard probe and hyperpolarized xenon. The *in vivo* extension can be envisioned in localized spectroscopy. On a dense tumor, spatial selection

of a region where a given cell line predominates should enable its analysis *via* the ^{129}Xe NMR spectrum.

14.3 Xenon in Functionalized Host Systems

Using hyperpolarized xenon alone as a sensor for biological cells requires, however, a homogeneous magnetic field. Except for some cells, such as RBCs or cyanobacteria, the low frequency difference between the signals of xenon in the bulk and in the cell compartment should not enable direct *in vivo* use. Furthermore, even if the previous paragraph and very recent developments show that a significant contrast can be observed on endogenous xenon host systems such as cells, gas vesicles[14] and spores,[15] where there is a large number of low-to-intermediate affinity sites, to date none of these systems is able to target specific biological receptors. Therefore, several molecular systems for which xenon develops a particular affinity and that give the noble gas a specific resonance frequency well resolved from the bulk signal, have been chemically decorated with biological ligands: microporous nanoparticles,[16] cage-molecules[17–20] and capsids.[21,22] The important parameters are the 'in' resonance frequency (that must be very different from the frequency of the bulk signal), the in–out xenon exchange (that must be slower than this frequency difference but fast enough to enable further gain in sensitivity), and the xenon binding constant (a high affinity is useful when the xenon/host concentration ratio is low).

Most of the biological sites/receptors and mechanisms that have been targeted so far after the proof-of-concept made on the avidin–biotin system[23] are enzymes[24,25] and cell-surface receptors.[26–28] The reason lies in the necessity to increase the local density of xenon hosts, using the catalytic cycle in the first case or the possible high number of receptors per cell and cell-internalization in the second case.

A biosensor proposed by Dmochowki *et al.* was based on a cryptophane-A linked to a RGD peptide.[29,30] The interaction of the biosensor with integrin induced a variation of the caged xenon frequency. Fluorescence of a Cy3 label showed internalization of the construct, but no ^{129}Xe spectrum of the biosensor in the cell was presented.

The spatial resolution obtained in classical MRI is not sufficient to enable distinction between the intra-cellular compartment and the bulk in ^{129}Xe MRI experiments. Therefore, in order to prove that targeting of cell-surface receptors was achieved, bimodal (fluorescence–^{129}Xe NMR) biosensors were conceived. Our group chose the transferrin system,[28] responsible for the transport of iron to cells, for several reasons. (i) Transferrin receptors are cell surface receptors which are internalized when transferrin is recognized. (ii) Some cells such as K562 erythroleukaemic cells exhibit a high number of receptors (more than 10^5). (iii) Labeling transferrin, an 80 kDa protein, by a small molecule (the cryptophane) is not expected to modify drastically the biological activity. (iv) The affinity of holo-transferrin for the receptor is 700 times higher than that of apo-transferrin, and obviously the presence of

the strongly paramagnetic Fe^{3+} ions could lead to fast xenon relaxation and could affect the sensitivity of the technique. But in case of a too drastic relaxation, iron ions could have been replaced by indium ions. (v) In our approach a cryptophane bearing an activated ester was synthesized. This enabled a non-specific (statistical) grafting of the cryptophane on some lysine residues of the protein (Figure 14.3a). Thus, various biosensors are easily built *via* this method.

Fluorescence microscopy showed the internalization of the biosensor in K562 cells (Figure 14.3b). After proper washing designed to separate the cells from the supernatant, the hyperpolarized ^{129}Xe NMR spectra were recorded.

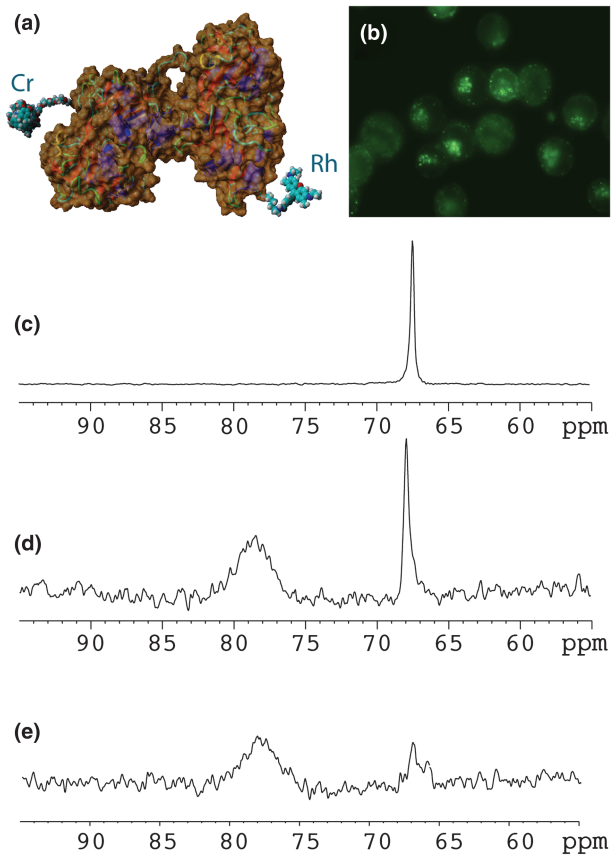

Figure 14.3 Cell internalization of a ^{129}Xe NMR-based biosensor. (a) Structure of the transferrin biosensor, where some cryptophane (Cr) and Rhodamine Green (Rh) moieties are non-specifically grafted on the Lys residues of the protein. (b) Fluorescence microscopy image of K562 cells incubated with this biosensor. (c)–(e) High field region of the ^{129}Xe spectra of (c) the transferrin biosensor in the supernatant, (d) the transferrin biosensor in the cell suspensions, (e) the BSA biosensor in the cell suspensions. Adapted from ref. 28.

The spectrum of the cell part is characterized by the presence of two signals at high field, separated by 10 ppm (Figure 14.3d). The first one (at 68 ppm) has the same chemical shift as the biosensor in the supernatant and the second peak represents the biosensor in the cell membrane. This indicates the internalization process of the transferrin biosensor even if the hydrophobicity of cryptophane induces a non-specific interaction of the probe with the plasma membrane of the cells. For comparison, a construct based on bovine serum albumin (BSA) was also designed. This protein was known to give rise to non-specific interactions with cells. After washing, the ^{129}Xe NMR spectrum of the cell part displayed the same signals but with a lower overall intensity and a ratio largely in favor of the membrane location (Figure 14.3e). This is in agreement with the fact that such a construct is internalized *via* pinocytosis.[31] This leads to the conclusion that although the transferrin biosensor is recognized and internalized by the cells, a part of the interaction occurs with the cell membrane, undoubtedly due to the hydrophobic character of the cryptophane.

Note that Klippel *et al.* recently used such a non-specific interaction of hydrophobic cryptophane moieties with the plasma membrane to perform MRI using the contrast between xenon in the free cage and xenon in the cage in interaction with the membranes for the purpose of cell-labeling.[32] Palaniappan *et al.* designed a biosensor where many cryptophanes are grafted on a bacteriophage expressing antibodies against EGFR (Epithelium Growth Factor Receptor).[26] They revealed, *via* HyperCEST, the specific interaction between the biosensor and the cell surface receptors.

14.4 Optimized Detection

The exchange of xenon between different environments, each having its own ^{129}Xe NMR spectral signature, is the advantage of the use of hyperpolarized xenon. It enables replenishment of the hyperpolarization after it has been destroyed by rf excitation or irradiation. Thus two methods can be used to detect the small reservoir constituted by xenon in cell (Xe@cell) or in a biosensor (Xe@host): directly with a series of soft pulses at the small reservoir frequency,[33] each followed by detection, or indirectly *via* detection of the variation of the bulk xenon signal after irradiation at the small reservoir frequency (HyperCEST[34]). The latter method has the advantage of being more sensitive, but the transient character of the hyperpolarization requires a continuous and homogeneous supply of polarized gas. Indeed except using normalization protocols, the lowest detectable amount of xenon in its host system or in the cell cannot be lower than the fluctuation level of supplied xenon magnetization.

As a way-around, we extended to xenon a method recently proposed to provide in one or two scans the whole Z-spectrum.[35] A field gradient applied during the rf irradiation enables saturation of the small reservoir in a region of the NMR tube. Detection performed in the presence of a second field gradient decodes to give the Z-spectrum (Figure 14.4).[36,37]

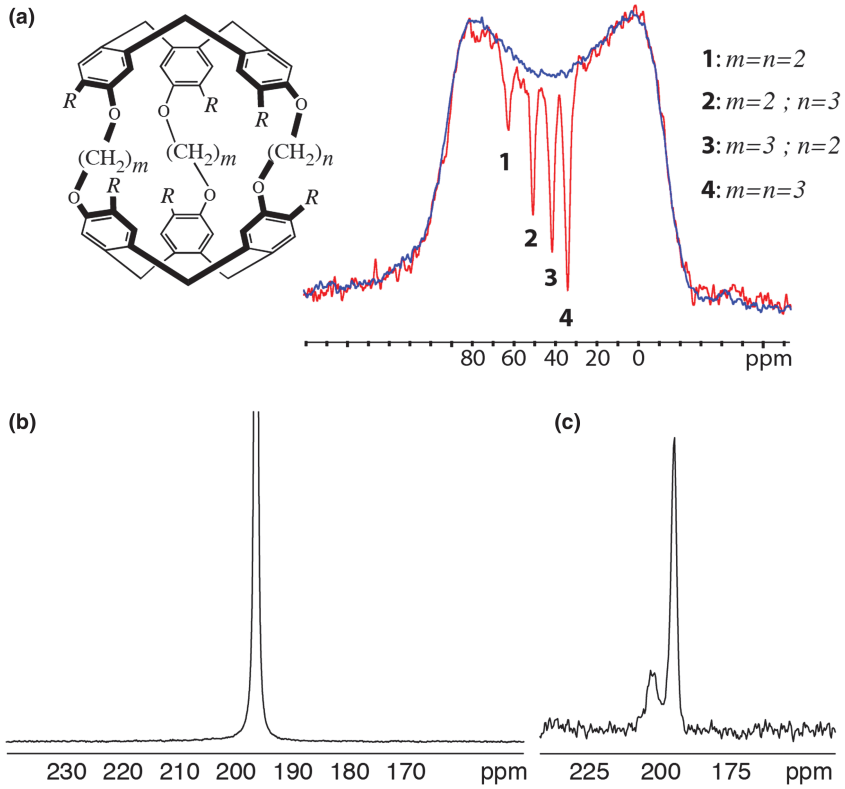

Figure 14.4 ^{129}Xe Ultrafast Z-spectroscopy. (a) Mixture of hexacarboxylated cryptophanes at 6 μM each, with CW saturation during 7.5 s at 2.4 μT (red) and without saturation (blue). (b)–(c) Sample of 25 million *S. cerevisiae* in 1.6 mL H_2O (estimated volume fraction 0.17%). (b) One-scan ^{129}Xe NMR spectrum; (c) Two-scan UFZ spectrum (8 s, $B_1^{sat} = 2.4$ μT).

Therefore, reliable results can be obtained even with significantly fluctuating xenon magnetization between pulses, and averaging can now be performed on a spectrum-by-spectrum basis (adding several UFZ-spectra to increase the signal-to-noise ratio). The robustness of UFZ toward magnetic field inhomogeneity is a further advantage of the approach.

14.5 Concluding Remarks

These few examples reveal how hyperpolarized xenon can be a potent probe of intra-cellular processes. In our laboratory these research efforts will be continued by (i) still reducing the number of cells needed for detection with help of micro-fluidics and micro-detection, (ii) developing the concept of a 'smart' probe, where a signal transduction inside the cell induces a xenon frequency shift. Several issues remain unresolved: what is the bio-distribution of xenon inside the cells that gives rise to such chemical shift

variations? Is it possible to transfer the xenon polarization to some metabolites in the cells? There is no doubt that future years will see a keen interest in the use of polarized xenon for the study of biological cells.

References

1. T. Pietrass and H. C. Gaede, *Adv. Mater.*, 1995, **7**, 826.
2. M. S. Albert, V. D. Schepkin and T. F. Budinger, *J. Comput. Assist. Tomogr.*, 1995, **19**, 975.
3. A. Bifone, Y. Q. Song, R. Seydoux, R. E. Taylor, B. M. Goodson, T. Pietrass, T. F. Budinger, G. Navon and A. Pines, *Proc. Natl. Acad. Sci. U. S. A.*, 1996, **93**, 12932.
4. M. S. Albert, D. Balamore, D. F. Kacher, A. K. Venkatesh and F. A. Jolesz, *NMR Biomed.*, 2000, **13**, 404.
5. C. Boutin, H. Desvaux, M. Carrière, F. Leteurtre, N. Jamin, Y. Boulard and P. Berthault, *NMR Biomed.*, 2011, **24**, 1264.
6. C. Boutin and P. Berthault, Procédé de détermination de la résistance cellulaire aux médicaments, 2012, FR2988857, http://www.directorypatent.com/FR/2988857.
7. B. C. Baguley, *Mol. Biotechnol.*, 2010, **46**, 308.
8. H. Sun, E. Chow, S. Liu, Y. Du and K. Pang, *Expert Opin. Drug Metab. Toxicol.*, 2008, **4**, 395.
9. P. Twentyman, T. Rhodes and S. Rayner, *Eur. J. Cancer*, 1994, **30A**, 1360.
10. S. E. Bates, Z. Zhan, J. Regis and E. Gamelin, *Methods Mol. Med.*, 1999, **28**, 63.
11. J. Le Gal, H. Morjani and M. Manfait, *Cancer Res.*, 1993, **53**, 3681.
12. C. Boutin, Y. Roche, C. Millot, R. Deturche, P. Royer, M. Manfait, J. Plain, P. Jeannesson, J. Millot and R. Jaffiol, *J. Biomed. Opt.*, 2009, **14**, 034030.
13. P. Winckler, A. Cailler, R. Deturche, P. Jeannesson, H. Morjani and R. Jaffiol, *Biochim. Biophys. Acta*, 2012, **1818**, 2477.
14. M. G. Shapiro, R. M. Ramirez, L. J. Sperling, G. Sun, J. Sun, A. Pines, D. V. Schaffer and V. S. Bajaj, *Nat. Chem.*, 2014, **6**, 629.
15. Y. Bai, Y. Wang, M. Goulian, A. Driks and I. J. Dmochowski, *Chem. Sci.*, 2014, **5**, 3197.
16. F. Lerouge, O. Melnyk, J. O. Durand, L. Raehm, P. Berthault, G. Huber, H. Desvaux, A. Constantinesco, P. Choquet, J. Detour and M. Smaïhi, *J. Mater. Chem.*, 2009, **19**, 379.
17. P. Berthault, G. Huber and H. Desvaux, *Prog. Nucl. Magn. Reson. Spectrosc.*, 2009, **55**, 35.
18. T. Brotin and J. P. Dutasta, *Chem. Rev.*, 2009, **109**, 88.
19. T. Adiri, D. Marciano and Y. Cohen, *Chem. Commun.*, 2013, **49**, 7082.
20. B. S. Kim, Y. H. Ko, Y. Kim, H. J. Lee, N. Selvapalam, H. C. Lee and K. Kim, *Chem. Commun.*, 2008, **24**, 2756.
21. T. Meldrum, K. L. Seim, V. S. Bajaj, K. K. Palaniappan, W. Wu, M. B. Francis, D. E. Wemmer and A. Pines, *J. Am. Chem. Soc.*, 2010, **132**, 5936.

22. T. Stevens, K. Palaniappan, R. Ramirez, M. Francis, D. Wemmer and A. Pines, *Magn. Reson. Med.*, 2013, **69**, 1245.
23. M. M. Spence, E. J. Ruiz, S. M. Rubin, T. J. Lowery, N. Winssinger, P. G. Schultz, D. E. Wemmer and A. Pines, *J. Am. Chem. Soc.*, 2004, **126**, 15287.
24. J. A. Aaron, J. M. Chambers, K. M. Jude, L. Di costanzo, I. J. Dmochowski and D. W. Christianson, *J. Am. Chem. Soc.*, 2008, **130**, 6942.
25. J. M. Chambers, P. A. Hill, J. A. Aaron, Z. Han, D. W. Christianson, N. N. Kuzma and I. J. Dmochowski, *J. Am. Chem. Soc.*, 2009, **131**, 563.
26. K. K. Palaniappan, R. M. Ramirez, V. S. Bajaj, D. E. Wemmer, A. Pines and M. B. Francis, *Angew. Chem., Int. Ed.*, 2013, **52**, 4849.
27. A. Schlundt, W. Kilian, M. Beyermann, J. Sticht, S. Günther, S. Höpner, K. Falk, O. Roetzschke, L. Mitschang and C. Freund, *Angew. Chem., Int. Ed.*, 2009, **48**, 1.
28. C. Boutin, A. Stopin, F. Lenda, T. Brotin, J. P. Dutasta, N. Jamin, A. Sanson, Y. Boulard, F. Leteurtre, G. Huber, A. Bogaert-Buchmann, N. Tassali, H. Desvaux, M. Carrière and P. Berthault, *Bioorg. Med. Chem.*, 2011, **19**, 4135.
29. G. K. Seward, Q. Wei and I. J. Dmochowski, *Bioconjugate Chem.*, 2008, **19**, 2129.
30. G. K. Seward, Y. Bai, N. S. Khan and I. J. Dmochowski, *Chem. Sci.*, 2011, **2**, 1103.
31. F. Pinaud, S. Clarke, A. Sittner and M. Dahan, *Nat. Methods*, 2010, **7**, 275.
32. S. Klippel, J. Döpfert, J. Jayapaul, M. Kunth, F. Rossella, M. Schnurr, C. Witte, C. Freund and L. Schröder, *Angew. Chem., Int. Ed.*, 2014, **53**, 493.
33. P. Berthault, A. Bogaert-Buchmann, H. Desvaux, G. Huber and Y. Boulard, *J. Am. Chem. Soc.*, 2008, **130**, 16456.
34. L. Schröder, T. J. Lowery, C. Hilty, D. E. Wemmer and A. Pines, *Science*, 2006, **314**, 446.
35. X. Xu, J.-S. Lee and A. Jerschow, *Angew. Chem., Int. Ed.*, 2013, **52**, 8281.
36. C. Boutin, E. Léonce, T. Brotin, A. Jerschow and P. Berthault, *J. Phys. Chem. Lett.*, 2013, **4**, 4172.
37. J. Döpfert, C. Witte and L. Schröder, *ChemPhysChem*, 2014, **15**, 261.